Chemical Engineering Journal 101 (2004) 379–390

Chemical Engineering Journal

www.elsevier.com/locate/cej

Flow distribution in different microreactor scale-out geometries and the effect of manufacturing tolerances and channel blockage

C. Amador, A. Gavriilidis, P. Angeli*

Department of Chemical Engineering, University College London, Torrington Place, London WC1E 7JE, UK

Received 31 July 2003; accepted 28 November 2003

Abstract

High throughput microreaction systems require a large number of microchannels operating in parallel (scale-out/number-up). Manifold structures should ensure the same residence time in all microchannels for operations involving heat/mass transfer and reactions. In this paper, flow distribution has been studied for two different manifold structures, namely consecutive and bifurcation, using a method based on electrical resistance networks. The method is validated against finite element simulations. The analytical model developed can be applied to both circular and rectangular channels and is used to study the effects of manufacturing tolerances and of channel blockages on flow distribution. Guidelines are drawn on the suitability of the manifold structures studied under different operating conditions, fabrication constraints and design objectives, based on their ability to produce narrow residence time distributions in the microchannel reactors.

Keywords: Flow distribution; Scale-out; Microreactor; Tolerance; Blockage

1. Introduction

The thin fluid layers present in microchannel reactors allow fast and controlled heat and mass transfer rates. For increased throughput, however, a number of such reactors operating in parallel is needed (scale-out or number-up). This type of scale up would ensure that findings from a single microchannel unit apply to the whole scaled out device, provided that the flow conditions in each channel are similar. Appropriate manifold structures are therefore needed to distribute the flow from a common reactant reservoir through the microchannels to a common product reservoir in a way that maintains the same residence time in all microchannels. Mean residence time in a microchannel together with temperature and pressure determine conversion and selectivity of reactions.

Commenge et al. [1] analysed flow distribution in a multichannel microreactor with a consecutive type of manifold and optimised the reactor design for single-phase flow distribution. A resistance network method combined with an optimising function was used to calculate the varying diameters of flow distributing and collecting channels that give almost uniform flow distribution while avoiding unrealistic channel geometries. Bejan and Errera [2] found that a fractal tree-like network structure (observed widely in natural structures such as cracks in a dry ground, lungs, arteries or veins and urban growth) not only gave flow uniformity but also minimised flow resistance through a *volume-to-point path* in a porous medium for a single-phase fluid. Yongping and Cheng [3] concluded that fractal tree-like microchannel networks have better heat transfer capabilities and require lower pumping power in comparison to traditional parallel channels; in this work, however, additional pressure losses due to bends that can appear at higher velocities were neglected. In contrast, in monoliths the flow expansion at the inlet cone leads to vortex formation that restricts the flow uniformity [4,5].

For the design of manifold structures that ensure uniform flow distribution, the equations describing flow in each microchannel need to be known. Researchers have questioned whether flow equations from large-scale systems can be used in micron size channels. In a recent review Judy et al. [6] showed that Stokes flow theory predicted friction factors well in laminar flow while deviations were within the experimental uncertainties due to the difficulty in conducting experiments at this scale, which would explain previous discrepancies between theory and experiments. In case of gas flow inside microchannels, rarefaction phenomena may appear at Knudsen numbers ($Kn = \lambda/D_C$) larger than 0.01, which represent very small channels (e.g. argon at 25 °C

* Corresponding author. Tel.: +44-(0)-207-679-3832; fax: +44-(0)-207-383-2348.
E-mail address: p.angeli@ucl.ac.uk (P. Angeli).

1385-8947/$ – see front matter © 2004 Elsevier B.V. All rights reserved.
doi:10.1016/j.cej.2003.11.031

Nomenclature

A	channel cross-sectional area (m^2)
b	maximum bifurcation level
d/c	distributing/collecting
D	hydraulic nominal diameter (m)
D_C	characteristic length. The smallest dimension of the reaction channels (nominal diameter in circular channels and nominal depth or width in rectangular ones) (m)
E	channel depth (m)
f	friction factor
FD	divergence from flow equipartition (%)
Kn	Knudsen number
L	channel length (m)
N	number of reaction channels
P	pressure (Pa)
ΔP	pressure drop (Pa)
P_0	reference pressure (Pa)
PAR	parameters determining the flow distribution solution
Q	flow rate (m^3/s)
R	frictional channel resistance ($Pa\,s/m^3$)
Re	Reynolds number
S, V	$S = 2(j-1)2^{b-i}+1$, $V = 2j2^{b-i}$; first and last reaction channel in the bifurcation manifold that contributes to the close loop j ($j = 1, \ldots, 2^i/2$) of level i
sep	nominal separation between reaction channels (m)
t	mean residence time in a channel (s)
U	fluid velocity (m/s)
W	channel width (m)

Subscripts

A	distributing channel
B	collecting channel
Bif	bifurcation
C	characteristic dimension
Consec	consecutive
EQ	equivalent property
EQUI	property under flow equipartition
Exp	experimental
m	mean value
MAX	maximum value
Nom	nominal value
R	reaction channel
T	total quantity of property entering the structure

Superscripts

#	dimensionless variable

Greek letters

δ	construction tolerance or channel dimensional variation (m)
λ	molecular mean free path (m)
λ_{NC}	non-circularity coefficient
μ	viscosity (kg/m s)
σ	sample standard deviation (%)

and atmospheric pressure has $\lambda = 0.07\,\mu m$ [7], giving $D_C = 7\,\mu m$).

In the present work, flow distribution in two different types of structures is studied using an analytical model analogous to electrical resistance networks [8]. This approach was chosen since it allows a large number of manifold structure geometries to be evaluated in less time than with computational fluid dynamics (CFD) simulations. The two structures studied are: (a) consecutive and (b) bifurcation (see Fig. 1). The analysis is restricted to single-phase laminar flow, commonly occurring in microscale, constant density and viscosity along the whole structure and no change of moles in gaseous reactions but can be extended to include these cases. It is also assumed that the fluid behaves as a continuum and pressure drop can be calculated by the equations used in large-scale flows. Compared to the fractal tree-like structure where the channels at the last level have the smallest length and diameter, in the bifurcation structure (Fig. 1b) the reaction channels (last level channels) are usually the longest ones.

2. Analytical model

To study flow distribution in a manifold structure the concept of an electrical resistance network is used. This is possible under laminar flow conditions where the relationship between frictional pressure drop ΔP and flow rate Q (or velocity U) in each channel is linear [1] and additional pressure losses at entrance, exit, bends and branching/merging of channels are negligible at low Reynolds numbers, Re. For laminar flow in circular channels the Hagen–Poiseuille equation can be used to estimate pressure drop for a given velocity U [9]. In non-circular channels, however, the channel hydraulic diameter, D (four times the channel area over wetted perimeter), combined with a non-circularity factor, λ_{NC}, that depends on channel geometry need to be included in the Hagen–Poiseuille equation for pressure drop [1]. This approach is used in this work and the Hagen–Poiseuille equation becomes:

$$\Delta P = \frac{32\mu L\lambda_{NC}}{D^2}U = \frac{32\mu L\lambda_{NC}}{D^2 A}Q \quad (1)$$

For non-dimensionalising Eq. (1) the smallest dimension of the reaction channels is chosen as characteristic length, D_C (i.e. nominal diameter in circular channels and nominal

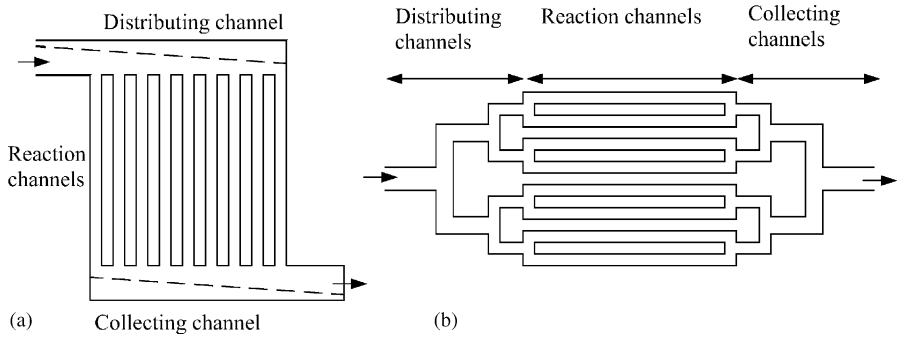

Fig. 1. Schematic diagrams of (a) consecutive and (b) bifurcation manifold structures. Consecutive manifold shows two possible designs: Method 1 (—) and Method 2 (- - -).

depth or width in rectangular ones), while the flow rate in each reaction channel when the flow is uniformly distributed (*equipartition flow rate* for identical reaction channels) is chosen as characteristic flow rate $Q_C = Q_T/N$. The characteristic area is defined as $A_C = \pi D_C^2/4$ for both circular and rectangular channels and the characteristic velocity is $U_C = 4Q_T/(N\pi D_C^2)$. The following dimensionless parameters are used: $L^\# = L/D_C$, $D^\# = D/D_C$, $W^\# = W/D_C$, $E^\# = E/D_C$, $A^\# = A/A_C$, $Q^\# = Q/Q_C$, $U^\# = U/U_C$, $Q_T^\# = N$ and dimensionless residence time and pressure are given by Eqs. (2) and (3), respectively (# denotes dimensionless parameter):

$$t^\# = \frac{tU_C}{D_C} = \frac{L^\#}{U^\#} \tag{2}$$

$$P^\# = \frac{(P - P_0)D_C}{\mu U_C} \tag{3}$$

where P_0 is a reference pressure. From dimensional analysis Eq. (1) becomes Eq. (4) and in circular channels the dimensionless resistance is given by Eq. (5). In Eq. (4) pressure difference is equivalent to potential difference and flow rate is equivalent to current in Ohm's law:

$$\Delta P^\# = R^\# Q^\# \tag{4}$$

$$R^\# = \frac{32L^\#}{D^{\#4}} \tag{5}$$

In non-circular channels, the non-circularity coefficient λ_{NC} can be found from the experimental values of the product fRe (equal to 64 in circular channels) obtained from pressure drop measurements (see Eq. (6)) [6]. However, there are available equations for the most common geometries [1,6] together with exact solutions for creeping flow [10].

$$\lambda_{NC} = \tfrac{1}{64}(f\,Re)_{Exp} \tag{6}$$

In rectangular channels, Eq. (7) is used to calculate the non-circularity coefficient λ_{NC} when $0 \le E/W \le 1$ while W/E is replaced by E/W when $E/W \ge 1$ [1].

$$\lambda_{NC} = \frac{3/2}{(1 - 0.351E/W)^2(1 + E/W)^2}, \quad 0 \le \frac{E}{W} \le 1 \tag{7}$$

Considering the hydraulic diameter $D = 2EW/(E + W)$ and area $A = WE$, Eq. (1) becomes Eq. (4) for rectangular channels as well, where the dimensionless resistance is now defined by Eq. (8) or (9), the latter being more useful for comparisons with circular channels:

$$R^\# = \frac{3\pi L^\#}{\min^2(E^\#, W^\#)(1 - 0.351\min(E^\#/W^\#, W^\#/E^\#))^2 W^\# E^\#} \tag{8}$$

$$R^\# = \frac{32\pi L^\# \lambda_{NC}}{D^{\#4}(E^\#/W^\# + W^\#/E^\# + 2)} \tag{9}$$

Manifolds with different geometries can be compared when the corresponding reaction channels have the same cross-sectional area so that the residence time in the channels remains constant (if the length is not modified). The smaller dimension of a rectangular channel of a given aspect ratio that has the same cross-sectional area as a circular one of diameter D is given by the following equation:

$$\min(E, W) = \left(\pi \min\left(\frac{E}{W}, \frac{W}{E}\right)\right)^{0.5} \frac{D}{2} \tag{10}$$

2.1. Resistance network for consecutive structure

The consecutive structure depicted in Fig. 1a is converted to the resistance network shown in Fig. 2 that contains $(N - 1)$ loops and N reaction channels.

In this configuration the distributing and collecting channels are divided into N zones, where each zone represents the distance between two reaction channels plus the reaction channel width (see patterned zones in Fig. 3). In the N-channel consecutive structure in Fig. 2, $R_{R,j}$, $R_{A,j}$ and $R_{B,j}$ are the flow resistances at channel or zone j ($j = 1$ to N) for reaction, distributing and collecting channels, respectively. If pressure drop is balanced in each loop (*loop rule*), the following $(N - 1)$ equations are obtained:

$$\begin{aligned} &Q_{A,(j+1)}R_{A,(j+1)} + Q_{R,(j+1)}R_{R,(j+1)} \\ &\quad - Q_{B,(N-j+1)}R_{B,(N-j+1)} - Q_{R,j}R_{R,j} = 0, \\ &j = 1, 2, \ldots, (N - 1) \end{aligned} \tag{11}$$

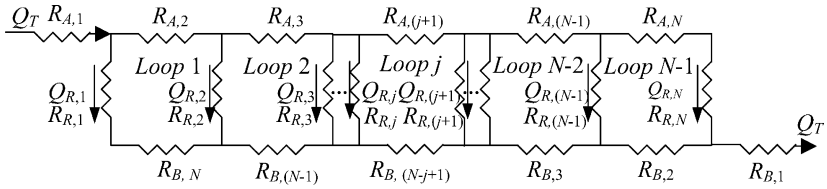

Fig. 2. Resistance network for consecutive structure.

$Q_{A,(j+1)}$ and $Q_{B,(N-j+1)}$ represent flow rates in zones $(j+1)$ and $(N-j+1)$ of the distributing and collecting channels, respectively, and can be expressed as a function of the reaction channels' flow rates by applying mass balances at each junction (*junction rule*):

$$Q_{A,(j+1)} = \sum_{k=1}^{k=N} Q_{R,k} - \sum_{k=1}^{k=j} Q_{R,k} \tag{12}$$

$$Q_{B,(N-j+1)} = \sum_{k=1}^{k=j} Q_{R,k} \tag{13}$$

Substituting Eqs. (12) and (13) into Eq. (11), non-dimensionalising and dividing throughout by $R^{\#}_{R,j}$ gives $(N-1)$ equations represented by Eq. (14) for loop j. An overall mass balance produces the Nth expression of the linear system of N-equations, Eq. (15), necessary to solve the flow distribution $Q^{\#}_{R,j}$ ($j = 1$ to N). The system can be expressed and solved in a matrix form where the coefficients of the matrix are calculated from the ratios of resistances $R^{\#}_{A,(j+1)}/R^{\#}_{R,j}$, $R^{\#}_{B,(N-j+1)}/R^{\#}_{R,j}$, $R^{\#}_{R\text{ and }(j+1)}/R^{\#}_{R,j}$ for $j = 1$ to $(N-1)$, which together with N, the number of reaction channels, gives $3(N-1)+1$ parameters (*PAR*) that determine the flow distribution solution. Resistances $R^{\#}_{A,1}$ and $R^{\#}_{B,1}$ do not affect flow distribution.

$$-\sum_{k=j+1}^{k=N} Q^{\#}_{R,k}\frac{R^{\#}_{A,(j+1)}}{R^{\#}_{R,j}} + \sum_{k=1}^{k=j} Q^{\#}_{R,k}\frac{R^{\#}_{B,(N-j+1)}}{R^{\#}_{R,j}} - Q^{\#}_{R,(j+1)}\frac{R^{\#}_{R,(j+1)}}{R^{\#}_{R,j}} + Q^{\#}_{R,j} = 0,$$
$$j = 1, 2, \ldots, (N-1) \tag{14}$$

$$\sum_{k=1}^{k=N} Q^{\#}_{R,k} = Q^{\#}_{T} = N \tag{15}$$

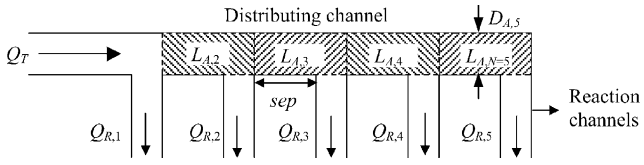

Fig. 3. Zone length and diameter in the distributing channel.

However, if all reaction channels are identical ($R^{\#}_{R,j} = R^{\#}_{R}$), *PAR* becomes $2(N-1)+1$ and if the distributing and collecting channels are also the same ($R^{\#}_{A,j} = R^{\#}_{B,j}$), $PAR = (N-1)+1$. Moreover, when all zones in distributing and collecting channels have the same geometry ($R^{\#}_{A,j} = R^{\#}_{B,j} = R^{\#}_{A}$), $PAR = 2$, namely R_A/R_R and N. The actual ratios of channel dimensions can be extracted from these ratios of resistances according to Eqs. (5) and (8) for circular and rectangular channels, respectively. To calculate resistances $R^{\#}$ from Eq. (5) or (8), the length of each j-zone in the distributing and collecting channels, $L^{\#}_{A,j}$ and $L^{\#}_{B,j}$ ($j = 2$ to N), is defined according to Eq. (16) for circular channels and Fig. 3, which shows a distributing channel with constant diameter. The same equation can be used for rectangular channels where channel width is used instead of diameter. Varying widths for the distributing and collecting channels are also possible where the zone width is taken equal to the average value along its length [1].

$$L^{\#}_{A,j} = L^{\#}_{B,j} = sep^{\#} + D^{\#}_{R,j}, \quad j = 2, 3, \ldots, N \tag{16}$$

2.2. Resistance network for bifurcation structure

Fig. 4 represents the resistance network for the bifurcation structure shown in Fig. 1b, where each bifurcation generates a new bifurcation level i. The bifurcation structure produces flow equipartition when all channels at the same level have exactly the same geometrical characteristics, the length of the straight channel after each bend is sufficient to develop a symmetrical velocity profile (1 to 10 times the channel diameter for Re between 1 and 400 in 2D) and there is no variation in the channel diameters due to manufacturing tolerances. This structure, however, tends to occupy larger area compared to the consecutive one. The inlet and outlet channels belong to level 0 and their resistances do not affect flow distribution but only the total pressure drop. The last bifurcation level ($i = b$) corresponds to the reaction channels. The number of reaction channels at the last level ($i = b$) is given by $N = 2^b$ and the number of channels in a lower bifurcation level i is given by 2×2^i, as there is the same number of channels at each side of the reaction channels. The channels at each i-level are numbered from top to bottom, from 1 to 2×2^i, starting from the left side and continuing to the right side. If the number of a channel in the left side is j, the number of its symmetrical channel in the right side is $j + 2^i$. The flow rate Q_{ij} ($i < b$) through channel number j at level i, is the sum of the reaction channel flow rates that

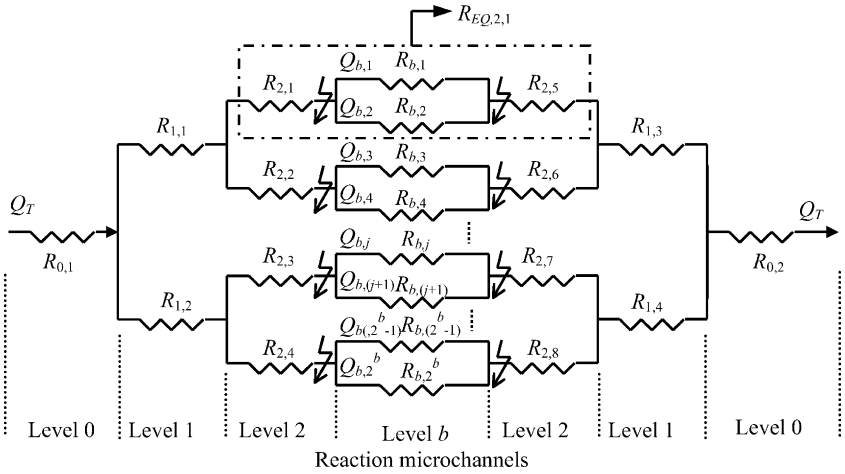

Fig. 4. Resistance network for bifurcation structure.

go from number $(j-1)2^{b-i}+1$ to $j2^{b-i}$. For instance, in a three-level structure $Q_{1,2}$ is the contribution of $Q_{3,5}$, $Q_{3,6}$, $Q_{3,7}$ and $Q_{3,8}$. The flow rate of its symmetry channel to the right side, $Q_{1,4}$ is the same. Resistance $R^{\#}_{i,j}$ (channel j at level i) is found by Eq. (5) or (8). The network can be simplified by the use of equivalent resistances given by Eqs. (17) and (18) for j resistances in series or in parallel, respectively:

$$R^{\#}_{\mathrm{EQ}} = \sum_j R^{\#}_j \tag{17}$$

$$\frac{1}{R^{\#}_{\mathrm{EQ}}} = \sum_j \frac{1}{R^{\#}_j} \tag{18}$$

At level i, there are 2^i equivalent resistances, which are numbered from top ($j=1$) to bottom ($j=2^i$). Eq. (19) is used to calculate equivalent resistances at level $i<b$. At level b, $R^{\#}_{\mathrm{EQ},b,j} = R^{\#}_{b,j}$. Fig. 4 shows the area that corresponds to the equivalent resistance $R_{\mathrm{EQ},2,j}$ as a dash-dot rectangle:

$$R^{\#}_{\mathrm{EQ},i,j} = \frac{R^{\#}_{\mathrm{EQ},(i+1),j} R^{\#}_{\mathrm{EQ},(i+1),(j+1)}}{R^{\#}_{\mathrm{EQ},(i+1),j} + R^{\#}_{\mathrm{EQ},(i+1),(j+1)}} + R^{\#}_{i,j} + R^{\#}_{i,(j+2^i)},$$
$$i = 1, 2, \ldots, (b-1), \quad j = 1, \ldots, 2^i \tag{19}$$

Applying mechanical energy and mass balances (loop and junction rules), the following system of $N-1 = 2^b - 1$ linear equations is obtained:

$$\sum_{k=S}^{k=(S+V-1)/2} Q^{\#}_{b,k} \frac{R^{\#}_{\mathrm{EQ},i,(2j-1)}}{R^{\#}_{\mathrm{EQ},i,2j}} - \sum_{k=((S+V-1)/2)+1}^{k=V} Q^{\#}_{b,k} = 0,$$
$$i = 1, 2, \ldots, b, \quad j = 1, \ldots, \frac{2^i}{2} \tag{20}$$

where level i goes from 1 to b, and loop j goes from 1 to $2^i/2$, which is the number of close loops in each level (equations). The number of close loops or equations per level is a quarter of the number of channels per level when $i<b$ and half the number of channels per level when $i=b$. S and V are given by $S = 2(j-1)2^{b-i}+1$ and $V = 2j2^{b-i}$. An overall mass balance similar to Eq. (15) with $N = 2^b$ gives the Nth equation of the system of N linear equations that can be expressed and solved in matrix form. The number of parameters determining the flow distribution solution for this structure is $PAR = (2^b - 1) + 1$ and is defined by the ratios $R_{\mathrm{EQ},i,(2j-1)}/R_{\mathrm{EQ},i,2j}$ ($i = 1$ to b and $j = 1$ to $2^i/2$) and the variable N. In this structure for same channel geometry at each level, sufficient straight channel length after each bend to ensure symmetrical velocity profile and in the absence of dimensional channel variations, flow equipartition is always achieved.

2.3. Overall pressure drop through the microstructure

At steady state, any flow path in the manifold gives the total pressure drop through the structure. Eq. (21) applies for the consecutive structure ($Q^{\#}_{\mathrm{T}} = N$) while for the bifurcation one, the total resistance is calculated by Eq. (22) and the total pressure drop via Eq. (23):

$$\Delta P^{\#}_{\mathrm{T,Consec}} = Q^{\#}_{\mathrm{T}}(R^{\#}_{\mathrm{A},1} + R^{\#}_{\mathrm{B},1}) + Q^{\#}_{\mathrm{R},N} R^{\#}_{\mathrm{R},N} + \sum_{j=1}^{N-1} \left(Q^{\#}_{\mathrm{T}} - \sum_{k=1}^{j} Q^{\#}_{\mathrm{R},k} \right) R^{\#}_{\mathrm{A},(j+1)} \tag{21}$$

$$R^{\#}_{\mathrm{T}} = R^{\#}_{0,1} + R^{\#}_{0,2} + \frac{R^{\#}_{\mathrm{EQ},1,1} R^{\#}_{\mathrm{EQ},1,2}}{R^{\#}_{\mathrm{EQ},1,1} + R^{\#}_{\mathrm{EQ},1,2}} \tag{22}$$

$$\Delta P^{\#}_{\mathrm{T,Bif}} = Q^{\#}_{\mathrm{T}} R^{\#}_{\mathrm{T}} \tag{23}$$

2.4. Manufacturing tolerances and channel blockages

Differences in the microstructure dimensions from the nominal sizes (*tolerances*) depend on the manufacturing process and feature size and can vary with direction [11]. *Micro-electrodischarge machining* (μ-EDM) has typical

manufacturing variations of 3–6 μm [11,12], which depend on channel length and aspect ratio. In case of parallel channels, the manufacturing variations could be minimised if the separation between two channels is greater than 200 μm. *Milling* gives a maximum difference of 10–20 μm between the engineering drawing and the milled channel [11,13]. This depends on the milling machine as well as on the accuracy of the milling head. If several parallel microchannels are fabricated, the differences between them are significantly smaller (approximately 5 μm). The fabrication variations using *etching* are mostly better than 20 μm, and depend substantially on the wafer material, channel aspect ratio and method [11]. Together with manufacturing variations, particle deposition, corrosion effects and irregular catalyst coating can also affect channel dimensions.

In order to study the effect of manufacturing tolerances and other channel dimensional variations on flow equipartition in manifolds, a maximum possible tolerance $\delta^{\#}_{\mathrm{MAX}}$ ($\delta_{\mathrm{MAX}}/D_{\mathrm{C}}$) is assumed that affects diameter ($\delta^{\#}_{\mathrm{D,MAX}}$) in circular channels and both width ($\delta^{\#}_{\mathrm{W,MAX}}$) and depth ($\delta^{\#}_{\mathrm{E,MAX}}$) in rectangular ones. If $T_{i,j}$, represents a $i \times j$ matrix with random numbers between 0 and 1, the tolerance matrix $\delta^{\#}_{i,j}$ that is applied to all channels in each structure for circular geometries is given by Eq. (24). Combining the tolerance matrix with that of the nominal diameter, $D^{\#}_{\mathrm{Nom},i,j}$ (see Eq. (25)), gives the real channel diameters that are within $D^{\#}_{\mathrm{Nom}} \pm \delta^{\#}_{\mathrm{D,MAX}}$. This implies constant tolerance along each channel. For rectangular channels, equations similar to Eqs. (24) and (25) are obtained for depth and width. If an increase in channel width also results in an increase in channel depth (same sign in all channels) not necessarily by the same amount but by the same percentage, the same $T_{i,j}$ matrix is used for both width and depth tolerances with $\delta^{\#}_{\mathrm{W,MAX}}$ and $\delta^{\#}_{\mathrm{E,MAX}}$, respectively. However, if depth and width tolerances vary independently, two different random $T_{i,j}$ matrices are used with $\delta^{\#}_{\mathrm{E,MAX}}$ and $\delta^{\#}_{\mathrm{W,MAX}}$, respectively. In the consecutive structure, i takes the values A for distributing, R for reaction and B for collecting channel and j refers to the channel or zone number ($j = 1$ to N). In the bifurcation structure i refers to the bifurcation level and j to the channel number at that level ($j = 1$ to 2×2^{i} except at last level $i = b$, where $j = 1$ to 2^{b}):

$$\delta^{\#}_{i,j} = T_{i,j}\, 2\delta^{\#}_{\mathrm{MAX}} - \delta^{\#}_{\mathrm{MAX}} \tag{24}$$

$$D^{\#}_{i,j} = D^{\#}_{\mathrm{Nom},i,j} + \delta^{\#}_{i,j} \tag{25}$$

In the consecutive structure, the length of the reaction channels is assumed to be unaffected by tolerances while the zone lengths in the distributing and collecting channels are found from Eqs. (26) and (27) for $j = 1$ to $(N - 1)$ in circular channels. The same equations can be applied to rectangular channels where channel width is used instead of diameter. In the bifurcation structure, all channel lengths are assumed to be unaffected by tolerances as they are several times the characteristic dimension D_{C}, and length also has a smaller effect than D_{C} on the pressure drop equation:

$$L^{\#}_{\mathrm{A},(j+1)} = sep^{\#} + D^{\#}_{\mathrm{R},(j+1)} + \tfrac{1}{2}(D^{\#}_{\mathrm{Nom}} - D^{\#}_{\mathrm{R},j}) + \tfrac{1}{2}(D^{\#}_{\mathrm{Nom}} - D^{\#}_{\mathrm{R},(j+1)}) \tag{26}$$

$$L^{\#}_{\mathrm{B},(N-j+1)} = sep^{\#} + D^{\#}_{\mathrm{R},(j+1)} + \tfrac{1}{2}(D^{\#}_{\mathrm{Nom}} - D^{\#}_{\mathrm{R},j}) + \tfrac{1}{2}(D^{\#}_{\mathrm{Nom}} - D^{\#}_{\mathrm{R},(j+1)}) \tag{27}$$

In order to simulate channel blockage, an infinite resistance in the blocked channel is applied.

2.5. Evaluation of flow distribution in manifold structures

In the absence of dimensional variations and for identical reaction channels, flow rate in each reaction channel is inversely proportional to residence time and both parameters can be used to indicate how good the flow distribution is. When dimensional variations are present, the reaction channels do not necessarily have the same cross-sectional area and equal flow rates in each channel will not result in the same residence times. Given its importance in processes involving mass/heat transfer and reaction, residence time instead of flow rate will be used to assess flow distribution in manifold structures when variations are present. Residence time for reaction channel $j = 1$ to N is given by the following equation:

$$t_{\mathrm{R},j} = \frac{L_{\mathrm{R},j}}{U_{\mathrm{R},j}} \rightarrow t^{\#}_{\mathrm{R},j} = \frac{L^{\#}_{\mathrm{R},j}}{U^{\#}_{\mathrm{R},j}} \tag{28}$$

As different reaction channels may have different flow rates, a linear mean of the residence times may not be realistic. An average value for the structure is obtained from the ratio of the total volume in reaction channels to the total flow rate entering the structure:

$$t_{\mathrm{m}} = L\sum_{j=1}^{N}\frac{A_{\mathrm{R},j}}{Q_{\mathrm{T}}} \rightarrow t^{\#}_{\mathrm{m}} = L^{\#}\sum_{j=1}^{N}\frac{A^{\#}_{\mathrm{R},j}}{N} \tag{29}$$

The standard deviation σ (%) of the residence time distribution in the reaction channels, which provides a measurement of the uniformity of flow distribution, is given by the equation:

$$\sigma\,(\%) = 100\sqrt{\frac{1}{N}\sum_{j=1}^{N}\left(\frac{t^{\#}_{\mathrm{R},j}}{t^{\#}_{m}} - 1\right)^{2}} \tag{30}$$

3. Results and discussion

3.1. Designs and criteria for uniform flow distribution in manifold structures in the absence of channel dimensional variations

When there are no dimensional variations, uniform flow distribution is always achieved in the bifurcation structure

where the channels at each level have the same size and the length of straight channel after each bend is sufficient for a symmetrical velocity profile to develop. In the consecutive structure, however, a proper design of the distributing and collecting (d/c) channels is required for flow equipartition and two different methods are analysed below. To characterise consecutive structure designs that do not result in equipartition, a divergence parameter *FD* (*Flow Distribution*) is used, defined by Eq. (31). In the absence of dimensional variations, where all reaction channels have the same length and area, *FD* is also very close to the maximum residence time divergence from the desired residence time in the reaction channels (e.g. a residence time divergence of 5.26% is obtained when $FD = 5\%$). Therefore, FD is used as a design parameter when tolerances do not play role:

$$FD\,(\%) = \max_{j=1}^{N}\left[100\frac{|Q_{\mathrm{EQUI}} - Q_{\mathrm{R},j}|}{Q_{\mathrm{EQUI}}}\right] = \max_{j=1}^{N}[100|1 - Q^{\#}_{\mathrm{R},j}|] \quad (31)$$

3.1.1. Method 1: uniform flow distribution via reduction of pressure drop in d/c channels—uniform cross-section d/c channels

In this approach pressure drop through the d/c channels is reduced compared to that in the reaction channels. This can be achieved if the d/c channels have a constant cross-section, larger than that of the reaction channels by a factor that depends on channel geometry, number and required degree of divergence from flow equipartition, *FD*. For zero divergence, zero pressure drop in the d/c channels is required. Therefore, considering the same geometry for the d/c zones ($PAR = 2$), Eqs. (14) and (15) are solved iteratively for different number of reaction channels *N* and different ratios of resistances R_R/R_A (equal to R_R/R_B) until the flow rate in each reaction channel diverges less than a certain *FD* (%). Fig. 5 shows results for four different *FD*: 1%, 2%, 5% and 10%. These results are valid for any channel geometry and it can be seen

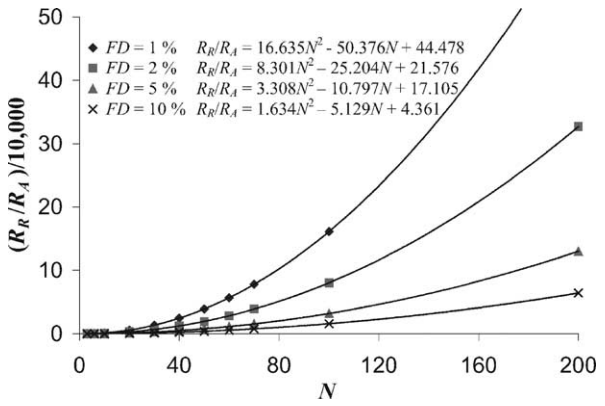

Fig. 5. Ratio R_R/R_A required for uniform flow distribution in the consecutive structure as a function of the number of reaction channels *N* and the divergence from flow equipartition *FD*.

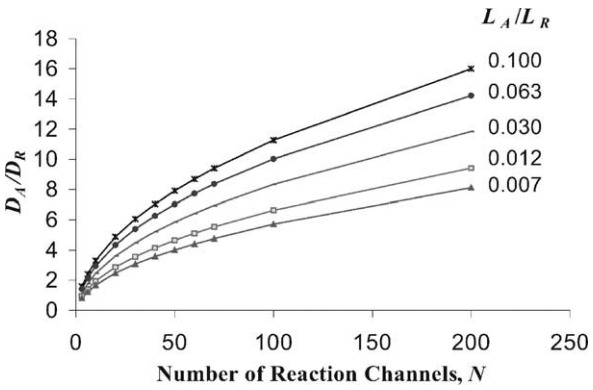

Fig. 6. Ratio D_A/D_R of circular channels required for uniform flow distribution ($FD = 1\%$) in the consecutive structure as a function of the number of reaction channels, *N*, and the length ratio L_A/L_R.

that a large ratio of resistances (or cross-sectional areas) is required for uniform flow distribution, especially for 1% divergence, which increases with the number of channels (i.e. for $N = 100$ and $FD = 1\%$, $R_R/R_A = 1.61 \times 10^5$).

From the above results for resistance ratios, the actual channel diameter and length ratios can be obtained for circular geometries from Eq. (5). The ratios of d/c to reaction channel diameters D_A/D_R are shown in Fig. 6 for 1% divergence from flow equipartition as a function of the ratio of zone length in d/c channels to reaction channel length, L_A/L_R and number of reaction channels, *N*. As the number of reaction channels *N* and the length ratio L_A/L_R increase, the required relative size of the d/c channels with respect to the reaction channels for flow equipartition increases. These results on flow distribution shown in Fig. 6 also apply to channels with rectangular cross-section when hydraulic diameters are considered and all channels in the structure have the same aspect ratio or the inverse one (see Eqs. (7) and (9)). This is feasible when different microchannel depths can be manufactured in the same substrate (i.e. anisotropic etching in silicon wafer [14]). However, when all channels have the same depth, Fig. 6 can still be used if the width/depth ratio of the d/c channels is made equal to the depth/width ratio of the reaction channels. This is achieved by using an intermediate depth between the reaction channel and the d/c channel widths. If the depth is equal to or smaller than the reaction channel width, Fig. 6 cannot be used anymore and the width of the d/c channels needs to be very large to obtain the required ratio R_R/R_A for flow equipartition (since the hydraulic diameter cannot be larger than double the minimum dimension). For any rectangular geometry (still $PAR = 2$), a similar graph to Fig. 6 can be obtained from Fig. 5 together with Eq. (8) where flow distribution would depend on five geometrical variables rather than three: (L_A/L_R, E_R/W_R, E_A/W_A, W_A/W_R and *N*).

Fig. 7 shows flow distribution in the reaction channels for two different hydraulic diameter ratios $D^{\#}_A = 1$ ($FD = 101.6\%$) and $D^{\#}_A = 3.44$ ($FD = 1\%$) for a 16-channel structure with length ratio $L_A/L_R = 0.04$ and square

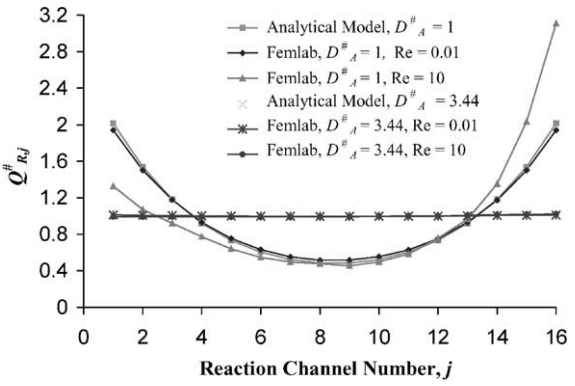

Fig. 7. Flow distribution in square channels obtained by the analytical model and the FEM simulations.

channels. Comparisons are also carried out using a commercial software (FEMLAB) based on the finite elements method (FEM) to solve the continuity and Navier Stokes equations for different Reynolds numbers, *Re*, taking into account the additional pressure losses neglected in the analytical model. The characteristic dimensions used in the *Re* definition are the same as those in the analytical model and gravity effects are neglected. Square channels rather than circular ones are chosen for this comparison as they give a better quality mesh in the FEMLAB simulations. The mesh is composed of 21,000 Lagrange-type second-order elements and an iterative algorithm is selected to solve the system of discretised equations. Two different Reynolds numbers, $Re = 0.01$ and 10, are used. The results from FEMLAB are very similar to those of the analytical model at low *Re*. Some discrepancies at higher *Re* and *FD* are probably due to the effect of additional pressure losses that are neglected in the analytical model. For this structure $FD = 5\%$ would reduce the required ratio $D^{\#}_{A}$ to 2.30.

If a rectangular channel structure is used with the same specifications as the one above (16 reaction channels, $L_A/L_R = 0.04$) and reaction channels with aspect ratio $E_R/W_R = 2$ (W_R is the characteristic dimension) where all channels have the same depth ($E^{\#}_{A} = E^{\#}_{B} = 2$), then for equal d/c and reaction channel widths $FD = 101.6\%$ is obtained (as above). The width of the d/c channels needs to be $W^{\#}_{A} = 25$ for $FD = 1\%$, which corresponds to a hydraulic diameter ratio of $D_A/D_R = 2.78$ instead of 3.44 (effect of non-circularity coefficient). However, $FD = 5\%$ is achieved for $W^{\#}_{A} = 6.01$. If the depth of all channels is reduced to $E^{\#} = 1$ with a reaction channels' aspect ratio $E_R/W_R = 1$, the width of the d/c channels for $FD = 1\%$ becomes very large, $W^{\#}_{B} = 59.5$.

3.1.2. Method 2: uniform flow distribution via equalisation of pressure drop in reaction channels—non-uniform cross-section d/c channels

In the second approach distributing and collecting channels are designed with gradually decreasing and increasing cross-sectional area, respectively, not necessarily linearly, in the flow direction. There is no size restriction for the d/c channel dimensions for flow equipartition but the actual size will define the total pressure drop and the effect of dimensional variations on flow distribution. This approach is the most suitable when the manifold area needs to be minimised and all channels must have the same depth, which in turn is similar to or smaller than the reaction channels' width. Commenge et al. [1] suggested an optimised design with non-linear d/c channels to limit the infinite solutions available for flow equipartition since some of them can give non-realistic geometries and flow recirculation patterns. Optimum linear d/c channels were also considered, which produce solutions close to flow equipartition in most cases.

If flow equipartition in a design with varying d/c channel diameters is assumed ($Q_{R,j} = Q_T/N$), the system of equations given by Eqs. (14) and (15) is simplified to $(N-1)$ independent equations, that relate the geometry of zone $(j+1)$ in the distributing channel to that of zone $(N-j+1)$ in the collecting one (see Eq. (32)):

$$R^{\#}_{A,(j+1)} = \frac{R^{\#}_{B,(N-j+1)}}{(N/j-1)}, \quad j = 1, 2, \ldots, (N-1) \qquad (32)$$

If therefore, the collecting channel geometry is known, the geometry of the distributing channel that produces flow equipartition can be found. When both d/c channels are symmetrical there are $(N-1)$ relationships given by $R^{\#}_{A,(j+1)} = R^{\#}_{B,(j+1)}$ which together with Eq. (32) only produce $(N-1)/2$ or $(N-2)/2$ independent relationships (depending on whether N is odd or even respectively), since Eq. (32) is the same for both $j = j$ and $j = (N-j)$. Therefore, for $(N-1)$ zones there are $(N-1)/2$ or $N/2$ degrees of freedom (either odd or even N, respectively) that produce infinite geometries for flow equipartition.

A simple method is suggested below for finding the exact geometry for perfect flow equipartition in such a structure with symmetrical d/c channels that occupy small area and have nearly linear diameter (or width) variation when the value of $D^{\#}_{B,N}$ (or $W^{\#}_{B,N}$ for rectangular channels) is given:

(A) Initially, the *optimum linear d/c channels* are obtained by calculating $D^{\#}_{B,2}$ that together with the given $D^{\#}_{B,N}$ produces linear d/c channels with the smallest divergence *FD* from flow equipartition. An initial guess for $D^{\#}_{B,2}$ is found assuming perfect flow equipartition from Eq. (32) when $R^{\#}_{A,(j+1)} = R^{\#}_{B,(j+1)}$ ($D^{\#}_{B,1}$ does not influence the flow distribution). $D^{\#}_{B,2}$ needs to be readjusted until *FD* is minimised.

(B) Either the collecting or distributing channel, e.g. collecting channel, is then assumed to have linear geometry defined by points $(D^{\#}_{B,2}, 2)$ and $(D^{\#}_{B,N}, N)$: $D^{\#}_{B,(j+1)} = D^{\#}_{B,2} - (j-1)(D^{\#}_{B,2} - D^{\#}_{B,N})/(N-2)$. The geometry of the distributing channel is found by Eq. (32) for flow equipartition. This does not result in identical d/c channels but very similar, one linear (see Fig. 8) and the other slightly curved.

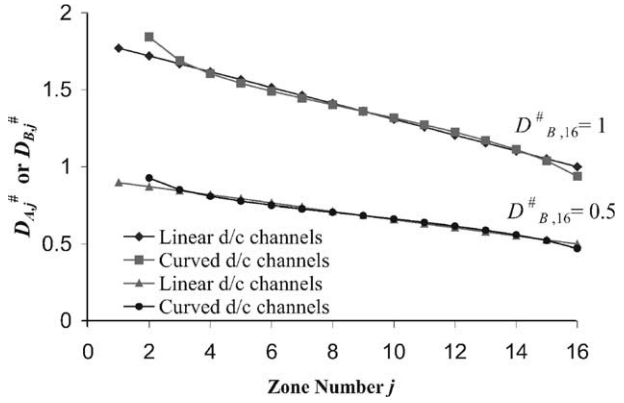

Fig. 8. Optimum linear and non-linear distributing (or collecting) channels in the consecutive structure for uniform flow distribution when initial $D^{\#}_{B,16} = 1$ and $D^{\#}_{B,16} = 0.5$.

(C) An intermediate geometry between the linear and the curved one, $D^{\#}_{B,(j+1)} = (D^{\#}_{A,(j+1)} + D^{\#}_{B,(j+1)})/2$, is used as a new geometry for the collecting channel, while from Eq. (32) the distributing channel geometry is recalculated, which in circular channels is the same as that of the collecting channel, resulting in symmetrical d/c channels (see Fig. 8). This geometry is the final one, in which the final value of $D^{\#}_{B,N}$ is not exactly the initial one but very close to it.

A similar procedure (but iterative in the last stage) can be applied to rectangular channels using channel widths rather than diameters. This simple method produces feasible geometries that are close to the optimum linear geometry, in just a few steps. Both the optimum linear and the non-linear d/c channel geometries for a 16 reaction channel structure with $L_A/L_R = 0.04$ are shown in Fig. 8 for two different initial values $D^{\#}_{B,16} = 1$ and $D^{\#}_{B,16} = 0.5$, which for the case of linear channels produce $FD = 1.90\%$ and 16.8%, respectively.

When using optimum linear d/c channels, the divergence from flow equipartition FD depends on the number of reaction channels, ratio of lengths $L_A/L_R = L_B/L_R$, aspect ratio in d/c zones and reaction channels and $D^{\#}_{B,N}$ (or $W^{\#}_{B,N}$ in rectangular channels). For a specific structure, FD can be improved by modifying the value of $D^{\#}_{B,N}$. For example, in a consecutive circular channel geometry with optimum linear d/c channels, length ratio $L_A/L_R = 0.04$, and diameter in the first collecting channel zone equal to that of the reaction channels ($D^{\#}_{B,N} = 1$), the divergence from flow equipartition is $FD = 1.90\%$ and 19.19% for 16- and 64-channel structures, respectively ($D^{\#}_{B,2}$ is 1.72 and 1.95). In the 64-channel structure $D^{\#}_{B,N} = 2.4$ ($D^{\#}_{B,2} = 4.45$) is required to reduce FD to 1%. In a rectangular channel structure, where all channels have the same depth, which in turn is similar to or smaller than the reaction channel width, the flow divergence for optimum linear d/c channels is much smaller. For instance, two 16- and 64-channel structures with rectangular channels, optimum symmetrical d/c channels and constant depth ($E^{\#}_{i,j} = 1$) with $L_A/L_R = 0.04$, $E_R/W_R = 1$ and $W^{\#}_{B,N} = 1$ produce $FD = 0.14\%$ and 0.33%, respectively, although larger widths are required for the d/c channels (i.e. $W^{\#}_{B,2} = 6.6$ and 24.1, respectively). However, this result is much better in relation to wafer area when compared to a uniform width of $W^{\#}_{B,j} = 59.5$ for the d/c channels obtained in the same 16-channel structure designed by Method 1.

3.2. Effect of manufacturing tolerances on flow distribution

In order to demonstrate the effect on flow distribution of manufacturing tolerances or changes in channel dimensions during a process, four 16-reaction channel manifold structures with circular channels are chosen (Designs A, B, C and D); three of them are consecutive, designed to give uniform flow distribution according to the previous section while the fourth one is based on bifurcation. Table 1 shows the dimensions of these designs (for Designs B and C see also Fig. 8).

In Fig. 9 the distribution of standard deviations of residence times, σ (%), and its mean value, σ_m (%), obtained after 10,000 runs, are shown for the four designs when $\delta^{\#}_{D,MAX} = 0.05$. The residence time variation in the reaction channels for the maximum standard deviation (worst case out of 10,000 runs) in each structure is shown in Fig. 10. Design B appears to have the largest mean standard deviation, which shows that although this design produces equipartition at any value of $D^{\#}_{B,N}$ in the absence of manufacturing

Table 1
Dimensions for Designs A, B, C and D, which are 16-channel structures with circular channels (see also Fig. 8 for Designs B and C)

	Design A	Design B	Design C	Design D
Type	Consecutive Method 1	Consecutive Method 2	Consecutive Method 2	Bifurcation
d/c channels	Uniform	Non-linear	Non-linear	Uniform
FD (%)	1	0	0	0
$D^{\#}_{A=B,j}$	3.44	–	–	–
$D^{\#}_{A=B,16}$	–	0.471	0.937	–
$D^{\#}_{i,j}$	–	–	–	1
$L^{\#}_{R,j}$	50	50	50	50
$L^{\#}_{A=B,1}$	10	10	10	–
$L^{\#}_{i,j}(i < b)$	–	–	–	10
$L_{A=B}/L_R$	0.04	0.04	0.04	–

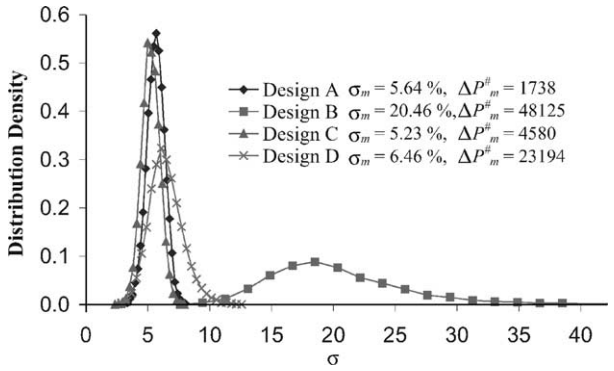

Fig. 9. Distribution of standard deviations of residence times in the reaction channels after 10,000 runs for Designs A, B, C and D.

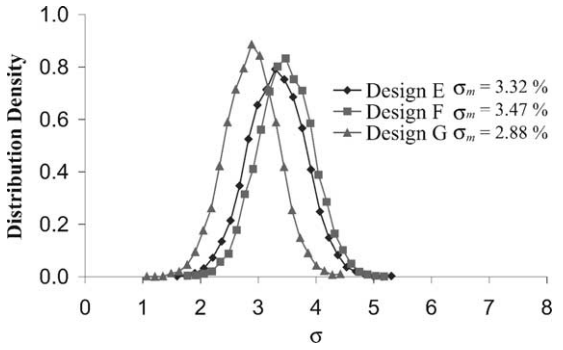

Fig. 11. Distribution of standard deviations of residence times in the reaction channels after 10,000 runs for Designs E, F and G.

variations, these can affect significantly the flow distribution at small $D^{\#}_{B,N}$. It is Design C that gives the lowest mean standard deviation. In Designs A and D even when the d/c channel resistances are completely removed (i.e. using very large diameter channels), $\sigma_m = 5.62\%$ is still higher than that of Design C, which indicates that d/c channel tolerances in Design C probably counteract the tolerances in the reaction channels themselves. Using $D^{\#}_{i,j} = 2$ in Design D for all channels except for the reaction channels ($D^{\#}_{R,j} = 1$) a similar effect occurs, $\sigma_m = 5.16\%$ ($\Delta P^{\#}_m = 2863$). Negative flow rates in some of the reaction channels (flow from the collecting to the distribution channel) can appear in the consecutive structures at large values of $\delta^{\#}_{D,MAX}$, mainly in those designed via Method 2 with small $D^{\#}_{B,N}$. For Design B the first negative flow rates appear at $\delta^{\#}_{D,MAX} = 0.10$. In Design C, negative reaction channel flow rates do not appear up to $\delta^{\#}_{D,MAX} = 0.55$. It is interesting to note that for Design A ($FD = 1\%$) in the presence of manufacturing tolerances, the mean standard deviation of the residence times is not very different if $FD = 5\%$ is used (in this case $\sigma_m = 6.14\%$). Thus, $FD = 5\%$ should be chosen as it only needs $D^{\#}_{A,j} = 2.3$ compared to $D^{\#}_{A,j} = 3.44$ for $FD = 1\%$.

In the above Designs B and C, non-linear collecting and distributing channels were used. If only linear d/c channels

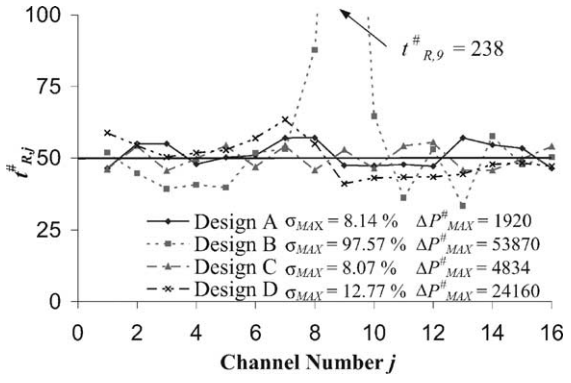

Fig. 10. Residence times in the reaction channels of Designs A, B, C and D for the worst scenario out of 10,000 runs.

are possible, flow rates will diverge from the equipartition flow rate ($FD = 19.19$ and 1.90%, respectively) while tolerances will further increase this divergence (Design B: $\sigma_m = 25.12\%$ and $\sigma_{MAX} = 90.77\%$; Design C: $\sigma_m = 5.43\%$ and $\sigma_{MAX} = 8.37\%$). Linear channels may be easier to manufacture but divergence from flow equipartition and effect of tolerances will depend on parameters such as $D^{\#}_{B,N}$, number of reaction channels N and length ratio and can be large. For example, the mean standard deviation in a 128-channel optimum linear structure with the rest of dimensions as Design C ($D^{\#}_{B,128} = 1$) is $\sigma_m = 65.44\%$ (design flow rate divergence, $FD = 38.88\%$).

As far as the total pressure drop through the manifold is concerned, the consecutive structure by Method 1 based on reducing pressure drop through the d/c channels gives the smallest mean value, $\Delta P^{\#}_m = 1738$. In the rest of the designs, pressure drop can be reduced by increasing the diameter of the d/c channels. In the bifurcation structure the channel flow rate increases as the bifurcation level decreases, and a gradual increase of the channel diameter with decreasing channel level would keep the pressure drop low.

In order to compare residence times in manifold structures with rectangular channels, these must have the same cross-sectional area (see Eq. (10)). If all channels are square, $\delta_{E,MAX}$ and $\delta_{W,MAX}$ are the same (or similar) and depth and width tolerances are positively proportional, i.e. a positive width tolerance produces a positive depth tolerance in each channel (e.g. KOH etching), the results will be similar to those shown in the circular channel analysis above. However, when d/c channels have a different aspect ratio from the reaction channels, there is a reaction channel aspect ratio that minimises the effect of tolerances for each $\delta_{E,MAX}/\delta_{W,MAX}$ ratio. Finally, when the depth and width tolerances in each channel are not related (e.g. milling), they have a counteracting overall effect and there is a reaction channel aspect ratio that minimises the effect of manufacturing variations as well. As an example of the last case, Fig. 11 shows distributions of the standard deviation of the residence times after 10,000 runs for three different 16-channel consecutive structures (Designs E, F and G) designed by Method 2 with optimum linear d/c channels where depth and width tolerances are not related and $\delta_{W,MAX} = \delta_{D,MAX}$ (the same value

Table 2
Dimensions for Designs E, F and G, which are 16-channel consecutive structures with rectangular channels designed by Method 2 with optimum linear d/c channels and same depth in all channels $E^{\#} = 1$

	Design E	Design F	Design G
Type	Consecutive Method 2	Consecutive Method 2	Consecutive Method 2
d/c channels	Linear	Linear	Linear
FD (%)	0.14	0.032	0.069
$E^{\#}_{i,j}$	1	1	1
$W^{\#}_{\mathrm{R},j}$	1	2	1.4
$W^{\#}_{\mathrm{B=A},16}$	1	2	1.4
$W^{\#}_{\mathrm{B=A},2}$	6.6	20.8	12.2
$L^{\#}_{\mathrm{R},j}$	56.42	79.79	66.76
$L_{\mathrm{A=B}}/L_{\mathrm{R}}$	0.04	0.04	0.04
$\delta_{\mathrm{W,MAX}}/\delta_{\mathrm{E,MAX}}$	2	2	2
$\delta^{\#}_{\mathrm{W,MAX}}$	0.0564	0.0798	0.0668

as that used for the circular channel case). Table 2 shows the dimensions of these designs. The absolute tolerances as well as lengths are the same in all designs although the dimensionless values are different. However, channel separation, *sep*, is slightly modified in order to keep the ratio $L_{\mathrm{A}}/L_{\mathrm{R}} = 0.04$. Design G with a reaction channel aspect ratio of 1.4 gives the smallest mean standard deviation.

3.3. Effect of channel blockages on flow distribution

Manufacturing defects, clogging processes due to particle deposition and bubbles trapped inside the channels can give rise to channel blockages. The response of manifold Designs A, B, C and D, used in the previous section, is now studied when one reaction channel (channel 1) is blocked. Fig. 12 shows the flow rate distribution in the reaction channels for each design. It can be seen that Design A reaches a new flow equipartition state with the flow rate of channel 1 equally distributed among the other channels. In the consecutive structures with varying diameters in the d/c channels (Designs B and C), flow equipartition is reached when the diameter of the d/c channels is sufficiently large.

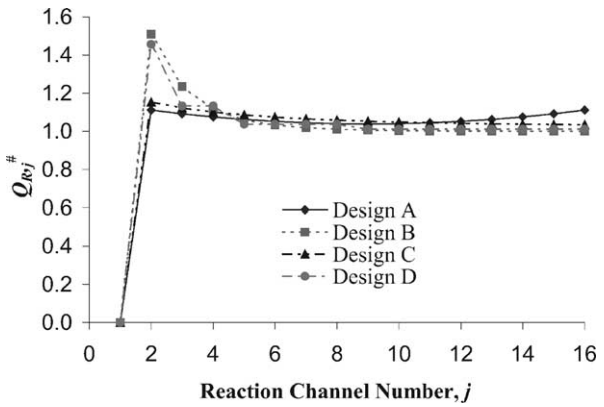

Fig. 12. Flow distribution in the reaction channels of Designs A, B, C and D when channel 1 is blocked.

As a result flow distribution improves significantly when $D^{\#}_{\mathrm{A},16}$ increases from 0.471 (Design B) to 0.937 (Design C). A similar situation could be reached in Design D if the diameter of the d/c channels was sufficiently large.

4. Conclusions

An analytical model based on resistance networks has been developed for the study of two manifold structures (consecutive and bifurcation) with different channel geometries. The model can take into account manufacturing variations randomly generated within specified tolerances as well as channel blockages at any part of the structure. The results from the analytical model compared well with those obtained from computational fluid dynamics simulations at low to moderate Reynolds numbers. However, the CFD simulations need time for the geometry and problem set-up, computation (from several minutes to hours at large channel numbers) and post-processing of the data, which in case of statistical or parametric studies where many cases would need to be run, may be large. With the analytical model only a few seconds were required to produce each line in Figs. 9 and 11 that consisted of 10,000 runs.

In the absence of channel dimensional variations the bifurcation structure always produces flow equipartition as long as the length of the straight channel after each channel bend is sufficient for a symmetrical velocity profile to develop. Two methods were considered for the design of the consecutive structure in order to achieve uniform flow distribution. Method 1 is based on minimising pressure drop in the distributing/collecting (d/c) channels by using a large enough uniform cross-section in the d/c channels (see Figs. 5 and 6). The reduction of pressure drop in d/c channels implies a small effect of channel dimensional variations and blockages and of additional pressure losses. Method 2 is based on equalising pressure drop in the reaction channels by using varying cross-sections in the d/c channels. The latter method can produce flow equipartition for any size of the d/c channels in the absence of channel dimensional variations if non-linear d/c channels are considered. In the case of linear d/c channels, the divergence from flow equipartition, *FD*, is generally small. However, similarly to designs by Method 1, when linear d/c channels are used in Method 2 an increase of reaction channel number, *N*, or length ratio of d/c to reaction channels, $L_{\mathrm{A}}/L_{\mathrm{R}}$, would require larger d/c channel cross-sections to keep the divergence *FD* low.

In addition, the analysis of the effect of channel dimensional variations and reaction channel blockages can give further insight on the performance of each design. When tolerances are present, the analytical model can help to identify the ratio of the d/c to reaction channel cross-sections that keep the standard deviation of the residence times, σ, in the reaction channels small. In rectangular channel structures a reaction channel aspect ratio can be found that minimises the effect of manufacturing variations on flow distribution.

Regarding the suitability of each manifold structure under different conditions the following can be concluded. The consecutive structure obtained by Method 1 is easy to design and fabricate (Fig. 5 applies to all designs irrespective of channel geometry and aspect ratio). This design is suitable when tolerances are large or uncertain, channel blockages are expected, different channel depths are possible or in case of constant channel depth, this is substantially larger than the reaction channel width. The consecutive structure obtained by Method 2 is suitable when tolerances are small or well-defined because they will affect the design value of the smallest dimension of the d/c channels. The designs obtained by Method 2 can be simplified using linear d/c channels, which in general produce a small divergence from flow equipartition. Method 2 is preferable when Method 1 is unfeasible or gives large d/c channel widths, which happens when all channels are etched with the same depth and the reaction channel depth is similar to or smaller than the reaction channel width (e.g. in the 16-channel structure analysed in Section 3.2 with constant channel depth equal to the reaction channel width, a 89% d/c channel width reduction is achieved using Method 2 compared to Method 1). The bifurcation structure is generally a good design and in the absence of channel dimensional variations it is the only one where flow distribution does not change for different flow rates Q_T at high *Re* where additional pressure losses become important. In the consecutive structures, a change in the flow rate at high *Re* produces a non-symmetrical change of the additional pressure losses due to bends and splits that would modify the flow distribution. This effect is generally small in designs by Method 1 (see Fig. 7) because the pressure drop in d/c channels is negligible, but can be significant in designs by Method 2. The bifurcation structure however, has two disadvantages: large area occupied by the d/c channels if *N* is large and many splits within each flow path, which together with longer d/c channels can increase the pressure drop (particularly important at higher flow rates).

In general, it can be said that the consecutive structure by Method 1 is more simple and safe than the others since information on tolerances and range of flow rates for low to moderate *Re* is not required for its design. Only when a constant depth is required, similar to or smaller than the reaction channel width, a consecutive design by Method 2 is better. At high *Re* additional pressure losses would need to be considered in the consecutive structures and a bifurcation structure may be preferable.

Acknowledgements

This project was sponsored by the European Commission (G1RD-CT2000-00469).

References

[1] J.M. Commenge, L. Falk, J.P. Corriou, M. Matlosz, Optimal design for flow uniformity in microchannel reactors, AIChE J. 48 (2002) 345–358.
[2] A. Bejan, M.R. Errera, Deterministic tree networks for fluid flow: geometry for minimal flow resistance between a volume and one point, Fractals 5 (1997) 685–695.
[3] C. Yongping, P. Cheng, Heat transfer and pressure drop in fractal tree-like microchannel nets, Int. J. Heat Mass Transfer 45 (2002) 2643–2648.
[4] M. Kostoglou, P. Housiada, G. Konstandopoulos, Multi-channel simulation of regeneration in honeycomb monolithic diesel particulate filters, Chem. Eng. Sci. 58 (2003) 3273–3283.
[5] S. Jeong, W. Kim, A study on the optimal monolith combination for improving flow uniformity and warm-up performance of an auto-catalyst, Chem. Eng. Proc. 42 (2003) 879–895.
[6] J. Judy, D. Maynes, B.W. Webb, Characterization of frictional pressure drop for liquid flows through microchannels, Int. J. Heat Mass Transfer 45 (2002) 3477–3489.
[7] Ch. Kloc, R.A. Laudise, Vapor pressures of organic semiconductors: α-hexathiophene and α-quaterthiophene, J. Cryst. Growth 193 (1998) 563–571.
[8] K. Golbig, S. Taghavi-Moghadam, P. Born, CYTOS^{TM} technology—microreaction technology in practical sense, in: Proceedings of the Sixth International Conference on Microreaction Technology, AIChE Spring Meeting, New Orleans, March 10–14, 2002, pp. 131–134.
[9] R.H. Perry, D.W. Green, Perry's Chemical Engineer's Handbook, 7th ed., McGraw-Hill, New York, Chapter 6, 1999.
[10] J. Happel, H. Brenner, Low Reynolds Number Hydrodynamics: With Special Applications to Particulate Media, Prentice-Hall, Englewood Cliffs, NJ, Chapter 2, 1965.
[11] IMM (Institut fuer Mikrotechnik Mainz), Germany, Private communication, 2003.
[12] G.L. Benavides, D.P. Adams, P. Yang, Meso-machining Capabilities, Sandia Report SAND2001-1708, June 2001.
[13] M.J. Madou, L.J. Lee, K.W. Koelling, S. Daunert, S. Lai, C.G. Koh, Y. Juang, L. Yu, Y. Lu, Design and fabrication of polymer microfluidic platforms for biomedical applications, in: Proceedings of the 59th Annual Technical Conference, vol. 3, Society of Plastic Engineers, 2001, pp. 2534–2538.
[14] O. Powell, B. Harrison, Anisotropic etching of {1 0 0} and {1 1 0} planes in (1 0 0) silicon, J. Micromech. Microeng. 11 (2001) 217–220.